

Backscatter Coefficient Estimation Bias under Acoustic Nonlinearities

Andres Coila, *Student Member, IEEE*, and Michael Oelze, *Member, IEEE*

Abstract—The backscatter coefficient (BSC) describes the scattering properties of a medium and can be used to characterize tissue. To calculate the BSC a calibration spectrum is required, which can be acquired using either a reference phantom method (RPM) or the planar reflector method (PRM). Although ultrasonic propagation is quasilinear at low acoustic pressures, for high acoustic pressures, acoustic nonlinear distortion becomes prevalent. Because water is low loss, use of the PRM method may introduce significant nonlinearities to the BSC estimation. In this study, we assessed the effects of the acoustic nonlinearities on BSC estimation when using the RPM and the PRM. Phantoms were scanned by exciting a single-element focused transducer ($f/2$) using one excitation level from low-power (LP) equipment (5800 PR, Panametrics Olympus, USA) and six excitation levels (EL1 to EL6) from high-power (HP) equipment (RAM-5000, Ritec, USA). This resulted in scanning the phantoms with increasingly higher pressures, but still within FDA limits for diagnostic ultrasound. The two phantoms, labelled phantoms A and B, had glass beads with diameters in the range 75-90 and 9-43 μm , respectively. The BSCs estimated with the LP system were used as a baseline. The normalized root-mean-squared error (RMSE) was calculated from BSCs estimated using the HP system with respect to the baseline. The BSC was parameterized to estimate the effective scatterer diameters (ESD) for each phantom using Faran's scattering theory. The BSC estimates resulted in smaller variations versus excitation levels for the RPM compared to the PRM. In the PRM, the RMSE was 0.62 ± 0.42 and 0.98 ± 0.77 for phantoms A and B, respectively; whereas, in the RPM, the RMSE was 0.21 ± 0.06 and 0.25 ± 0.12 for phantoms A and B, respectively. The ESD for the phantom A using the PRM decreased from 75 μm for EL1 to 39 μm for EL6; and using the RPM the ESD was 74.7 ± 2.3 μm across all settings. The ESD for the phantom B using the PRM decreased from 47 μm for EL1 to 0.5 μm for EL6; and using the RPM the ESD was 39.2 ± 5.6 μm across all settings. The RPM method was more robust against nonlinear distortion compared to the PRM because the PRM was used in water, where low loss resulted in large nonlinear distortion of the reference pulse.

Index Terms—Backscatter coefficient, quantitative ultrasound, nonlinearity parameter

I. INTRODUCTION

The backscatter coefficient (BSC) is a quantitative ultrasound parameter useful for tissue characterization [1], [2]. The BSC is a fundamental property of tissue, like the attenuation or sound speed. The BSC is calculated from ultrasonic backscattered signals and is an estimate of the

A. Coila and M. L. Oelze are with the Beckman Institute for Advanced Science and Technology, Department of Electrical and Computer Engineering, University of Illinois at Urbana-Champaign, IL, 61801, USA. e-mail: acoila@illinois.edu.

differential backscattered cross-section of the scatterers per unit volume. The BSC is often represented in the frequency domain providing the ultrasonic scattering power per frequency channel.

To obtain the BSC in practice, a reference spectrum is required to account for system effects. The two commonly used BSC reference methods are the planar reflector method and reference phantom method and assume linear acoustic propagation, which can be assumed for low acoustic pressures. Under an acoustic linear assumption, the BSC can be estimated after compensating for external effects, i.e., the system acquisition, the attenuation effects, and the beam diffraction [3], [4].

However, a linear acoustic propagation assumption may not be appropriate because acoustic propagation is inherently nonlinear [5] and nonlinearity might need to be accounted when high acoustic pressures are used (e.g., for increasing the SNR of the backscattered signals). A practical result of the acoustic nonlinear behavior is the generation of harmonics, i.e., acoustic energy is transferred from the fundamental frequency band to higher harmonics.

Therefore, we hypothesize that the BSC estimates using both methods: the planar reflector method and the reference phantom, might include a bias due to acoustic nonlinear distortion. Moreover, because in the planar reflector method a water path is used and water has low attenuation in the clinical ultrasonic frequency ranges (approximate two order of magnitude less attenuating than most soft tissues), the development of acoustic nonlinearity in water is expected to be encountered more readily than in soft tissues. The Gol'dberg number is larger for materials with high nonlinearity parameter (B/A) and low attenuation [6]. The larger the Gol'dberg number the more likely nonlinear distortion will be observed. In this work, we assessed two BSC estimation methods, i.e., the planar reflector method and the reference phantom method, using tissue-mimicking phantoms in the presence of acoustic nonlinear distortion. The nonlinear distortion is obtained through the use of large acoustic pressures, but still below the FDA exposure limits for diagnostic ultrasound [7], generated with a high power excitation system.

II. METHODS

A. BSC estimation methods

Two commonly used BSC estimation methods were assessed: the planar reflector method and the reference phantom method. The first method exploits the simple geometry

of the transducer to analytically compute the diffractive effects [3]. The second method can be used with more complex transducer geometries but can also increase the variance of estimates without sufficient ensemble averaging of the reference spectrum [4]. Figure 1 depicts the data acquisition for the BSC estimation methods.

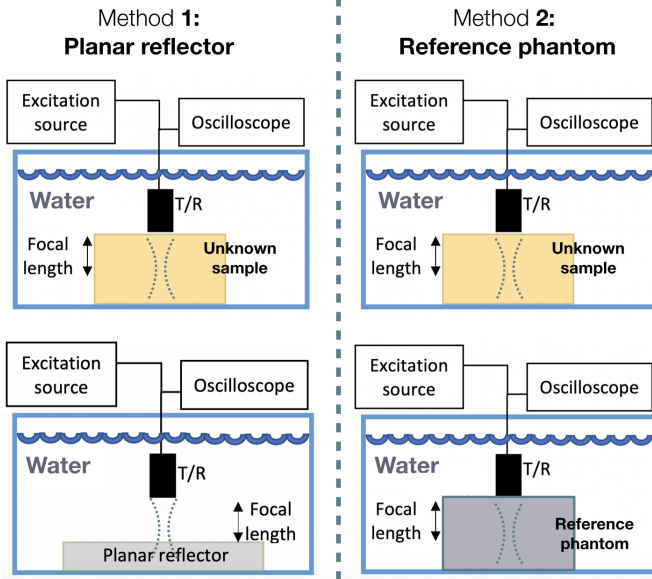


Fig. 1: RF acquisition setup. Left: Acquisition of backscattered signals around the focal region from the unknown sample and the planar reflector. Right: Acquisition of backscattered signals around the focal region from the unknown sample and the reference phantom.

1) *Planar reflector method*: The planar reflector method has been used with transducers having simple geometry, e.g., spherical focused transducers, because the effects of diffraction can be computed analytically and incorporated into the BSC calculation [3]. In this work, a spherically focused single-element transducer was used for BSC estimation. Gated scan lines of RF data from an interrogated medium corresponding to an axial length Δz and centered at the focal distance F , i.e., between $\langle F - 0.5\Delta z, F + 0.5\Delta z \rangle$, were recorded. The BSC, denoted by $\sigma(f)$, was computed from this data using equation (5) in [8]

$$\sigma(f) = 2.17D(G_p) \frac{\gamma^2 F^2}{\pi R^2 \Delta z} \frac{S(f, F)}{S_w(f, F)} A(f, F),$$

$$D(G_p) = |\exp(-iG_p)[J_0(G_p) + iJ_1(G_p)] - 1|^2, \quad (1)$$

where $S(f, F)$ is the power spectrum averaged over several gated scan lines estimated from a data block, $S_w(f, F)$ is the average power spectrum of reflected echoes from a planar reflector located at depths between $\langle F - 0.5\Delta z, F + 0.5\Delta z \rangle$, $A(f, F)$ compensates for the attenuating effects of unknown medium and water, R is the transducer radius, γ is the reflection coefficient of the planar reflector, $G_p = (kR^2)/(2F)$

is the focal gain and J_ν is the Bessel function of the first kind and order ν . In (1), the system effects are assumed to be cancelled in the ratio of the spectra $S(f, F)/S_w(f, F)$.

2) *Reference phantom method*: The system effects can also be compensated using a reference phantom method. Assuming equivalent speed of sound in both sample and reference phantom, the diffractive effects are compensated through measurements as opposed to theory. The reference phantom needs to be previously well characterized, i.e., its acoustic parameters such as sound speed, BSC and attenuation coefficient are known. The BSC from the sample is estimated as [4]

$$\sigma(f) = \sigma_{\text{ref}}(f) \frac{S(f, F)}{S_{\text{ref}}(f, F)} \frac{A_{\text{ref}}(f, F)}{A(f, F)}, \quad (2)$$

where $S(f, F)$ and $S_{\text{ref}}(f, F)$ are the averaged power spectra from data blocks located at the same depth in the sample and the reference phantom, respectively, $A(f)$ and $A_{\text{ref}}(f, F)$ are the attenuation compensation functions for the sample and reference phantom, respectively, and $\sigma_{\text{ref}}(f)$ is the known BSC of the reference phantom. In (2), the system effects are assumed to be canceled in the ratio of the power spectra $S(f, F)/S_{\text{ref}}(f, F)$.

B. Experimental setup

We scanned phantoms by exciting a single-element focused transducer ($f/2$, 0.5" diameter and 5-MHz center frequency, using one excitation level from low power equipment (5800 PR, Panametrics Olympus, USA) and six excitation levels (EL1 to EL6) from equipment capable of producing large pressure fields (RAM-5000, Ritec, USA). This resulted in scanning the phantoms with increasingly higher pressures (see Table I), but still within FDA limits for diagnostic ultrasound [7]. The transducer sampled the phantom at 121 locations for subsequent averaging of power spectra. Fig. 2 shows the waveform for the peak signal (measured with a needle hydrophone submerged in water) for the low power setting and a high power setting (specifically, the largest excitation level) to visualize the larger nonlinear distortion.

TABLE I: Summary of peak positive pressure and peak negative pressure values associated with the settings used in this study.

	Peak positive pressure (MPa)	Peak negative pressure (MPa)
Low Power		
Excitation level 1	0.66	0.75
High Power		
Excitation level 1	7.58	2.78
Excitation level 2	9.10	3.38
Excitation level 3	10.22	3.83
Excitation level 4	11.02	4.21
Excitation level 5	11.54	4.52
Excitation level 6	12.10	4.74

The two phantoms, labelled phantoms A and B, were constructed with an agar-milk matrix and glass beads with

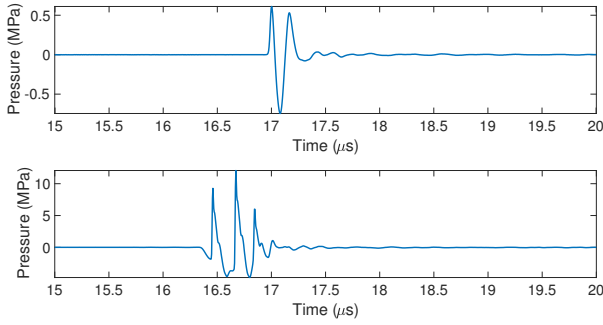


Fig. 2: Time domain representation of the waveforms at the focus for the low power (top) setting and high power setting for the largest excitation level (bottom) measured with a needle hydrophone.

diameters in the range 75-90 and 9-43 μm , respectively. Other parameters of the phantoms include the attenuation coefficient that was estimated by performing additional through transmission experiments and found to be $\alpha_A(f) = 0.41f^{1.15}$ dB/cm and $\alpha_B(f) = 0.79f^{1.05}$ dB/cm, respectively. The nonlinearity parameter (B/A) was assumed to be 6.6 ± 0.3 for the phantoms based on literature values for this type of phantom [9].

C. Metrics

1) *Root mean square error*: The normalized root mean square error between BSC estimates from different power settings was computed as

$$\text{RMSE}_x = \frac{\|\sigma_{\text{HP-x}}(f) - \sigma_{\text{LP}}(f)\|}{\|\sigma_{\text{LP}}(f)\|} \quad (3)$$

where the subscripts HP-x and LP correspond to the BSCs using high power setting x (with $x \in \{1, 2, \dots, 6\}$) and low power setting, respectively. The low power estimate of the BSC was used as a baseline reference.

2) *Effective scatterer diameter*: The ESD was estimated from the BSC by searching values of an effective scatterer radius, a_{eff} , that minimized the average squared deviation [10] between the estimated BSC and the BSC derived from Faran theory [11]. The properties of the glass beads used in Faran's theory calculation were: density, 2380 Kg/m³; speed of sound, 5572 m/s; Poisson's ratio, 0.21.

III. RESULTS

The BSC estimates obtained using the low power setting are shown in Fig. 3, which were used subsequently as baseline BSCs. Figure 4 show the BSC estimates using the high power settings with the planar reflector method (a), (c) and the reference phantom method (b), (d) for the phantoms A and B. In the reference phantom method, when estimating the BSC of the phantom A, the reference was the phantom B, and vice versa. Visually, the BSC estimates when using the

reference phantom method presented small deviations across the six excitation levels, whereas when using the planar reflector method, the BSCs had increasing slope with higher excitation levels. In the planar reflector method, the RMSE was 0.62 ± 0.42 and 0.98 ± 0.77 for phantoms A and B, respectively; whereas, in the reference phantom method, the RMSE was 0.21 ± 0.06 and 0.25 ± 0.12 for phantoms A and B, respectively.

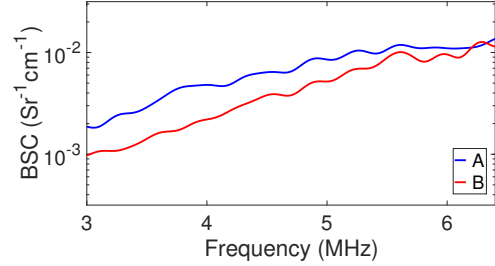


Fig. 3: BSCs from phantom A (blue) and B (red) when using the low power settings (planar reflector method). This BSC estimates were used as the baselines estimates.

The ESD for the phantom A using the planar reflector method decreased from 75 μm for EL1 to 39 μm for EL6; and using the reference phantom method the ESD held at 74.7 ± 2.3 μm across all settings. The ESD for the phantom B using the planar reflector method decreased from 47 μm for EL1 to 0.5 μm for EL6; and using the reference phantom method the ESD held at 39.2 ± 5.6 μm across all settings.

IV. DISCUSSION

We demonstrated in physical phantoms with similar acoustic properties to those found in soft tissues that the BSC estimates obtained using the reference phantom method had less sensitivity to nonlinear distortion than the planar reflector method. Therefore, the reference phantom method would be more suitable for BSC estimation when high amplitude pressures are used. In the planar reflector method, the nonlinear effects derived from the high power settings resulted in increasing deviations of the BSC estimates from the BSC estimated using the low power setting. Therefore, accuracy was reduced using the planar reflector method.

The ESD values were in better agreement with the expected sizes when using the reference phantom method. For example, in phantom B, the ESD values obtained for excitation settings larger than 2 using the planar reflector method were 0.5 μm , which was the minimum value possible. This occurred because the dependence of $\sigma(f)$ with frequency became larger than that of the Rayleigh scattering theory (f^4). Hence, the ESD estimates from BSCs obtained using the planar reflector method could result in inaccuracies for the tissue characterization task.

The results of the study suggest that to improve BSC estimate bias and variance, high ultrasonic powers can be

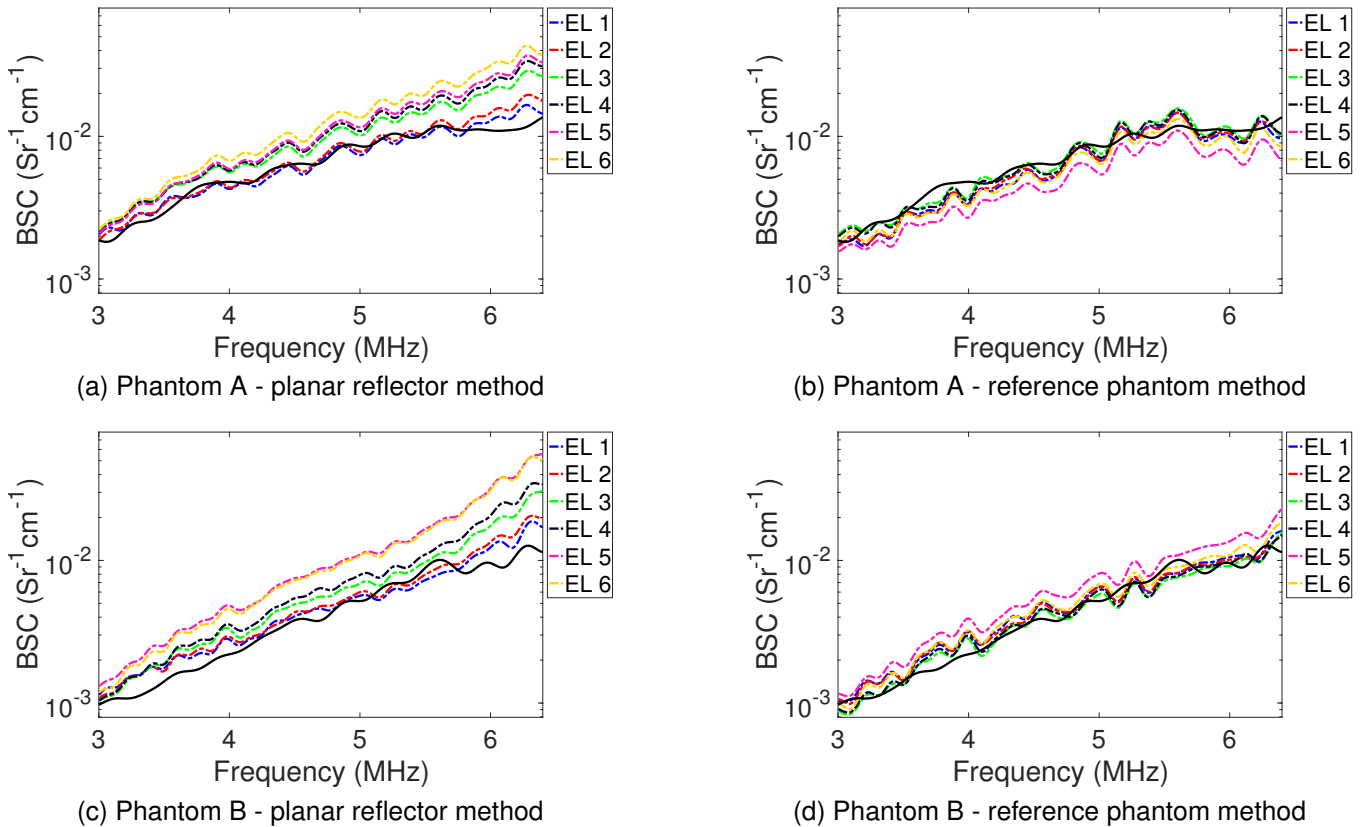


Fig. 4: BSC estimates from phantom A (top) and phantom B (bottom) when using the planar reflector method (left) and the reference phantom method (right) with high power settings (6 excitation levels). Solid lines are the baseline BSCs estimated using the low power settings (from Fig. 3).

used, but should be used with a reference medium that has nontrivial attenuating properties, i.e., not water.

In conclusion, the findings suggest that accuracy of the planar reflector method when using a water propagation path is more sensitive to nonlinear distortion effects than the reference phantom method, thus improving the consistency of the BSC for tissue characterization.

ACKNOWLEDGMENT

A. Coila acknowledges the financial support from the National Council of Science, Technology and Technological Innovation (CONCYTEC, Perú) through the National Fund for Scientific, Technological Development and Technological Innovation (FONDECYT, Perú) under grant 132-2016. The authors also acknowledge grants from the NIH (R21EB024133 and R21EB023403).

REFERENCES

- [1] J. Mamou and M. L. Oelze, *Quantitative ultrasound in soft tissues*. Springer, 2013.
- [2] M. L. Oelze and J. Mamou, "Review of quantitative ultrasound: Envelope statistics and backscatter coefficient imaging and contributions to diagnostic ultrasound," *IEEE transactions on ultrasonics, ferroelectrics, and frequency control*, vol. 63, no. 2, pp. 336–351, 2016.
- [3] X. Chen, D. Phillips, K. Q. Schwarz, J. G. Mottley, and K. J. Parker, "The measurement of backscatter coefficient from a broadband pulse-echo system: a new formulation," *IEEE Trans. Ultrason. Ferroelectr. Freq. Control*, vol. 44, no. 2, pp. 515–525, 1997.
- [4] L. X. Yao, J. A. Zagzebski, and E. L. Madsen, "Backscatter coefficient measurements using a reference phantom to extract depth-dependent instrumentation factors," *Ultrason. Imaging*, vol. 12, no. 1, pp. 58–70, 1990.
- [5] A. D. Pierce, *Acoustics: An Introduction to Its Physical Principles and Applications*. Melville, NY: Acoustical Society of America, 1989.
- [6] L. E. Kinsler, A. R. Frey, A. B. Coppens, and J. V. Sanders, *Fundamentals of Acoustics*. John Wiley & Sons, Hoboken, NJ, 4th ed., 2000.
- [7] T. L. Szabo, *Diagnostic ultrasound imaging: Inside out*. Elsevier Academic Press, 2004.
- [8] R. Lavarello, D. Phillips, K. Q. Schwarz, J. G. Mottley, and K. J. Parker, "The measurement of backscatter coefficient from a broadband pulse-echo system: a new formulation," *IEEE Trans. Ultrason. Ferroelectr. Freq. Control*, vol. 44, no. 2, pp. 515–525, 2011.
- [9] F. Dong, E. L. Madsen, M. C. MacDonald, and J. A. Zagzebski, "Nonlinearity parameter for tissue-mimicking materials," *Ultrasound Med. Biol.*, vol. 25, no. 5, pp. 831–838, 1999.
- [10] M. F. Insana, R. F. Wagner, D. G. Brown, and T. J. Hall, "Describing small-scale structure in random media using pulse-echo ultrasound," *J. Acoust. Soc. Am.*, vol. 87, no. 1, pp. 179–192, 1990.
- [11] J. J. Faran, "Sound scattering by solid cylinders and spheres," *J. Acoust. Soc. Am.*, vol. 23, no. 4, pp. 405–418, 1951.